

**THERMOPHYSICAL PROPERTIES OF SELECTED LUNAR STUDY REGIONS DETERMINED FROM LROC AND DIVINER DATA.** K. E. Bauch<sup>1</sup>, H. Hiesinger<sup>1</sup>, M. S. Robinson<sup>2</sup>, and F. Scholten<sup>3</sup>. <sup>1</sup>Institut für Planetologie, Westfälische Wilhelms-Universität, Wilhelm-Klemm-Str. 10, 48149 Münster, Germany. <sup>2</sup>School of Earth and Space Exploration, Arizona State University, Tempe, AZ 85251, USA. <sup>3</sup>DLR-Institut für Planetenforschung, Rutherfordstr. 2, 12489 Berlin, Germany. karin.bauch@uni-muenster.de.

**Introduction:** The thermal inertia of a surface is an important property for determining temperature variations of planetary surfaces [e.g. 1, 2]. It represents the ability of a subsurface to retain heat and is defined as a combination of thermal conductivity  $k$ , density  $\rho$  and heat capacity  $C$ :

$$I \equiv \sqrt{k\rho C} \quad (1)$$

Fine grained soil yields a low thermal inertia, and therefore quickly loses heat during the lunar night. Rocks and exposed bedrock yield higher thermal inertia values and store more heat during the night, which results in higher nighttime temperatures [2].

Using Diviner temperature data combined with subsets of the 100 m grid LROC WAC DTM (GLD100, [3]), we derived maps of thermal inertia for different study regions, such as Taurus-Littrow Valley, Aristarchus and Lichtenberg Crater.

**Method:** Diviner nighttime temperatures are used to estimate thermal inertia of the lunar surface. The data was binned in one hour intervals, at a minimum resolution of 32 pixels per degree. We use an expanded version of the thermal model presented by [4] to generate temperature curve look-up tables for various thermal inertia values including different local topography, layering, and time of the lunar day. For each surface facet, we compare measured and modeled temperature data in order to find the best fitting thermal inertia value. This approach is similar to Martian thermal inertia derivations described by [2, 5].

The thermal model solves the one dimensional heat transfer equation, where the surface boundary condition is based on the energy balance relation; the energy entering the surface equals the energy leaving the surface:

$$\frac{S_0}{R^2} \cos(i) (1 - A) + k \frac{\partial T}{\partial z} = \varepsilon \sigma T_0^4 \quad (2)$$

The first term is an insolation function, which includes the solar flux  $S_0$  at 1 AU, and the surface albedo  $A$ . The orbital radius  $R$  and solar inclination  $i$  are calculated from JPL's Horizons software and updated in each time step. The second term represents subsurface conduction and the last term radiation loss into space, including the soil's emissivity  $\varepsilon$  and Stefan-Boltzmann constant  $\sigma$ . The bottom layer boundary condition is given by a constant planetary heat flow from below.

**Study regions:** Taurus-Littrow Valley (20°N, 31°E, figure 1) on the southeastern edge of Mare Serenitatis was the landing site of the Apollo 17 mission.

This region is of special interest for thermal studies, because heat flow experiments have been performed during the mission and temperature data over the whole lunar cycles are available [6]. These data sets allow the derivation of a detailed model of the surface and subsurface thermophysical properties.

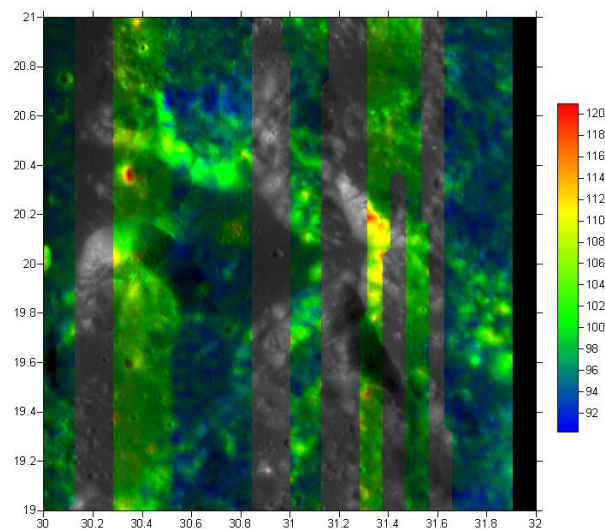


**Figure 1:** Diviner Channel 8 nighttime temperatures superposed on WAC-mosaic of Taurus-Littrow Valley. Temperatures are in K.

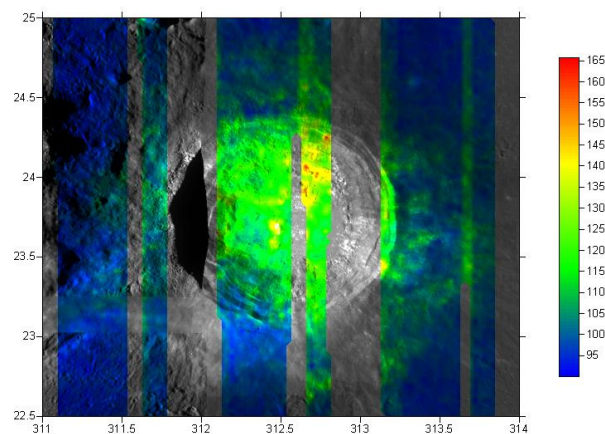


**Figure 2:** Diviner Channel 8 nighttime temperatures superposed on WAC mosaic of Aristarchus Crater. Temperatures are in K.

Aristarchus Crater is a ~ 40 km large crater (figure 2) located at 23.7°N, 312.6°E at the southeastern edge of the Aristarchus plateau within Oceanus Procellarum. Crater counts indicate that Oceanus Procellarum

contains the youngest lunar mare deposits [7]. NIR spectra reveal a diversity of compositions in the region around Aristarchus [8], which is one of the areas with the highest Thorium abundances [9].

Lichtenberg Crater is about 20 km in diameter (figure 3), located at 31.8°N, 292.3°E in the western part of Oceanus Procellarum. This crater presents a diverse geologic setting, with young basalts to the east, and older basalts with different composition in the north and west. The crater has an extensive ejecta blanket, with rays extending more than 100 km from the crater's rim [10].

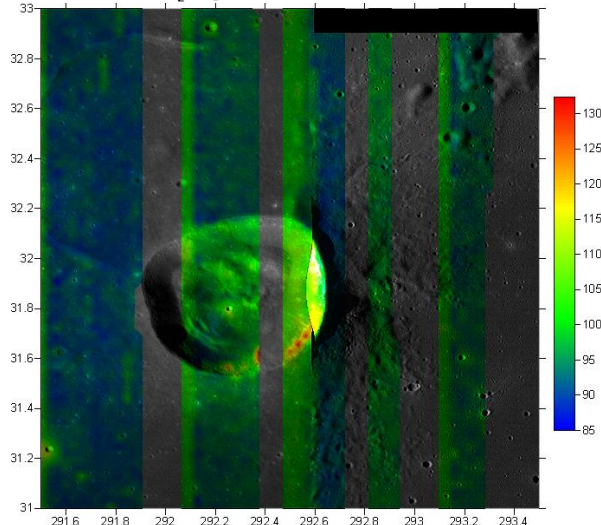


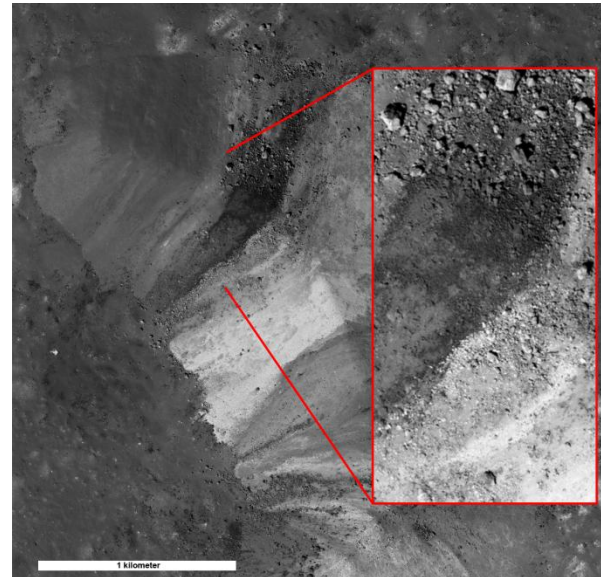
**Figure 3:** Diviner Channel 8 nighttime temperatures superposed on WAC-mosaic of Lichtenberg Crater. Temperatures are in K.

**Results:** Most of the area at Taurus-Littrow valley can be described by a layering subsurface model, with a very fine regolith having a low thermal inertia ( $\sim 20 \text{ Jm}^{-2}\text{K}^{-1}\text{s}^{-1/2}$  during the night) covering a more dense and conductive layer. This model is also in good agreement with a model obtained for the Apollo temperature measurements as described by [6]. The second layer on the floor of the valley has thermal inertia values  $< 100 \text{ Jm}^{-2}\text{K}^{-1}\text{s}^{-1/2}$  during the night. Due to the temperature dependence of thermal conductivity and heat capacity, the values are higher during the lunar day. The massifs surrounding the valley (Northern Massif, Sculptured Hills, and Southern Massif) and impact craters yield higher thermal inertia values ( $> 300 \text{ Jm}^{-2}\text{K}^{-1}\text{s}^{-1/2}$ ).

Temperatures measured on the ejecta blanket of Aristarchus crater can also be explained by a layered subsurface model. Temperatures decrease with distance from the crater, indicating finer material with increasing distance. Close to the crater thermal inertia of the second layer is  $< 200 \text{ Jm}^{-2}\text{K}^{-1}\text{s}^{-1/2}$ , with increasing distance thermal inertia decreases to less than  $100 \text{ Jm}^{-2}\text{K}^{-1}\text{s}^{-1/2}$ .

The floor of the impact crater is 30-35 K warmer than the ejecta blanket. High temperature anomalies are associated with the central peak, which is about 40 K warmer than ejecta blanket. Parts of the crater wall, in particular in the north-east, are up to 60 K warmer than the ejecta blanket. These areas suggest the presence of rocks and/or bedrock at or very close to the surface. This can be confirmed by high-resolution NAC-images, showing boulders of different sizes in these regions (figure 4).

**Figure 4:** Reduced resolution NAC mosaic of the



Aristarchus central peak, with 700 meter wide close-up; NAC M122523410 [NASA/GSFC/Arizona State University].

The ejecta blanket of Lichtenberg crater also shows evidence for low thermal inertia ( $< 100 \text{ Jm}^{-2}\text{K}^{-1}\text{s}^{-1/2}$ ). As for Aristarchus, high temperature anomalies are associated with the crater walls (figure 3). However, temperatures on the crater floor and walls are only 20 K and up to 40 K higher than the ejecta blanket, respectively. Ejecta blankets of both craters do not show evidence for large boulders or exposed bedrock.

**References:** [1] Urquhart, M.L. and Jakosky, B.M. (1997), *JGR* 102, 10,959-10,969. [2] Mellon, M.T. et al. (2000), *Icarus* 148, 437-455. [3] Scholten, F. et al. (2011), *LPSC XLII* (this conf.). [4] Bauch, K.E. et al. (2009), *LPSC XL*, Abstract #1789. [5] Putzig, N.E. et al. (2005), *Icarus* 173, 325-341. [6] Keihm, S.J. and Langseth, M. G., Jr. (1973), *Proc. Lunar Sci. Conf.* 4, 2503-2513. [7] Hiesinger, H. et al. (2003), *JGR* 108, 5065. [8] Lucey, P.G. et al. (1986), *JGR* 91, D344-D354. [9] Lawrence, D.J., et al. (2000), *JGR* 105, 20,307-20,331. [10] McAlpin, D.B. et al. (2008), *LPSC XXXIX*, Abstract #1443.